European Commission

JRC TECHNICAL REPORTS

Interpretation of maps on the assessment of the Human-Environment system productivity into dedicated land degradation maps

EUROCLIMA-JRC Desertification, Land Degradation and Drought (DLDD), and biophysical modelling for crop yield estimation in Latin America under a changing climate
Deliverable No. 1

Weynants M., Kutnjak H., Cherlet M.

2016

Joint Research Centre

EUR 28035 EN

Contact information
Michael Cherlet
Address: Joint Research Centre, Via Enrico Fermi 2749, TP044, 44/025
I-21027 Ispra (VA) - Italy

E-mail: michael.cherlet@jrc.ec.europa.eu
Tel.: +39 033278 9982

JRC Science Hub
https://ec.europa.eu/jrc

EUR 28035 EN

PDF ISBN 978-92-79-60680-9 ISSN 1831-9424 doi:10.2788/157180

Luxembourg: Publications Office of the European Union, 2016

How to cite: Weynants M., Kutnjak H., Cherlet M.; Interpretation of maps on the assessment of the Human-Environment system productivity into dedicated land degradation maps; EUR 28035 EN; doi:10.2788/157180

Contents

Acknowledgements

This work was developed under the EUROCLIMA programme funded by the European Union and managed by the Directorate General International Cooperation and Development - EuropeAid.
http://www.euroclima.org/en/
EUROCLIMA facilitates the integration of climate change mitigation and adaptation strategies and measures into Latin American public development policies and plans. The objectives are to contribute to poverty reduction of the Latin American population by reducing their environmental and social vulnerability to climate change and to reinforce resilience of the Latin America region to climate change and promote opportunities for green growth.
Within this programme, the Joint Research Centre (JRC) strengthens and disseminates knowledge on Desertification, Land Degradation and Drought (DLDD) and develops bio-physical and bio-economic models for agricultural systems and policy analysis for Latin America.

This work also supports the new edition of the World Atlas of Desertification (http://wad.jrc.ec.europa.eu).

We thank our JRC colleagues who provided material to this work. Hugo Carrão processed the drought data. Ilaria Palumbo processed the burned area data. Martino Pesaresi shared the Global Human Settlement Layer.

Abstract

Land degradation is a complex and multidimensional issue. Mapping active degradation at continental or global level is virtually impossible given the local scale of the processes involved. However, patterns of human-environment interactions that are likely to lead to land degradation can be identified. The combination of spatial(-ised) indicators of these patterns with land productivity dynamics derived from Earth observation can be interpreted to highlight places where land degradation may be ongoing. Further small scale investigation is needed to determine the gravity of the potential land degradation locally.

1 Introduction

Land degradation is defined by the FAO as the reduction in the capacity of the land to provide ecosystem services [1]. Ecosystem services are the benefits that humans gain from ecosystems [2]. They include provisioning (e.g. food; fuel; fibre; genetic resources; biochemical, natural medicines and pharmaceuticals; ornamental resources; fresh water), regulating (e.g.: air quality regulation; climate regulation; water regulation; erosion regulation; water purification and waste treatment; disease regulation; pest regulation; pollination; natural hazard regulation), cultural (e.g.: cultural diversity; spiritual and religious values; knowledge systems; educational values; inspiration; aesthetic values; social relations; sense of place; cultural heritage values; recreation and ecotourism) and supporting services (soil formation; photosynthesis; primary production; nutrient cycling; water cycling).
The United Nations Convention to Combat Desertification (UNCCD, www.unccd.int) defines desertification as land degradation in drylands, while

> *land degradation* means reduction or loss [...] of the biological or economic productivity and complexity of rainfed cropland, irrigated cropland, or range, pasture, forest and woodlands resulting from land uses or from a process or combination of processes, including processes arising from human activities and habitation patterns.

The three components of land degradation, which are biological productivity, economic productivity and ecosystem complexity, are not directly measurable. Indicators that describe them do not necessarily agree [3], which makes the assessment of land degradation subject to the interests of the expert or the considered stakeholders.
"Land degradation processes are highly dependent on a complex interaction between biophysical factors and land use systems, both of which vary in space and time [4]." Land degradation is difficult to assess at a continental or global scale given the local scale of the processes involved and the complex interactions between the local human actions and the environment. The importance of local land conditions (soil, geology, climate, land use and management) make the processes difficult to up-scale. Numerous local to regional studies and a few global initiatives have been published. Among them, the Global Assessment of Human-Induced Soil Degradation (GLASOD, 1987-1990) was a UNEP-funded project, conducted by ISRIC. It has produced a world map of human-induced soil degradation, using an approach based on expert knowledge [5]. More recently, the Land degradation assessment in drylands (LADA 2006-2010) was funded by the FAO. The project defined land degradation as the long-term decline in ecosystem function and measured it in terms of net primary productivity. In the global segment of LADA, the authors identified six tangible components of the ecosystem services on which pressures apply and result in degradation processes [6]: biomass, soil, water, biodiversity, economics and social. For each axis, they estimated the status and the degradation processes at play. They combined them into an indicator of land degradation. The reviewers of the project criticised the lack of validation and the choice of some of the datasets used as input. The authors argued that they did conduct local studies in some countries and that they used the state-of-the-art datasets freely available at the time. However at such a resolution (5 arc-minutes), the local processes cannot be assessed.
Gibbs and Salomon recently reviewed the global efforts assessing land degradation [7]. They distinguish four strategies: (1) Expert base, e.g. GLASOD, (2) Remote sensing based, e.g. temporal analysis of vegetation index in LADA [8], (3) Biophysical models, of which further work could advance the application to the assessment of land degradation by focusing on direct assessment of land vulnerability, rather than using marginality as a proxy, (4) Abandoned agricultural land mapping. As possible ways forward, they propose to focus on relevant and consistent definitions and to put emphasis on modes of degradation.
Particular interest should be given to indicators revealing slow but pernicious evolution of soil quality [9].

Concurring biophysical and societal process changes can be identified (at global scales) but need interpretations specific to the local context to define the trade-offs and identify solutions to improve the sustained provision of ecosystem services. Besides, the focus should not concentrate on the mapping of perceptions but on identifying what is needed to improve the situation.
In this study we propose to integrate global maps of the land system productivity dynamics (LPD), that mainly account for the biomass status and processes, with components of land degradation at a resolution of 30 arc-seconds (1 km at the equator). In the framework of EUROCLIMA-JRC, we focus the analysis on Latin America but the results are available at global scale.

We consider that the main driving forces of land degradation are intensive agriculture (mechanised, using excess fertilisers and unsustainable irrigation), overgrazing, urban and industrial development (land take and soil contamination), deforestation.

2 Looking for convergence of evidence

Land degradation cannot be mapped as such at global or continental scale. The processes involved are multiple and their interactions are driven by local conditions difficult to capture at that scale. Nevertheless one can look for convergence of evidence of regional conditions that are likely to translate into LD processes.
In this study, we use a map of the land productivity dynamics (LPD) obtained from phenological variables derived from Earth Observation data as an indicator of the direction and intensity of change in the vegetation productivity. We integrate this with other spatial(ised) data as indicators of the human-environment biophysical processes that can initiate, worsen or reverse land degradation. We construct indicators of the susceptibility to land degradation for four classes of land use: crop, pasture, forest and urban. For each, we identify and combine different factors that could constitute favourable grounds for land degradation. We interpret these in combination with the land productivity dynamics, including drought severity and fire occurrence in the analysis.

2.1 Land productivity dynamics

Building on numerous studies that use Normalised Difference Vegetation Index (NDVI) as base layer, a set of phenological metrics was calculated from time series of the vegetation index, providing additional information on various aspects of vegetation/land cover functional composition in relation to dynamics of ecosystem functioning and land use [10].
The methodology relies on the theory that the combination of weak evidence can converge into a stronger indicator. Evidence of direction and intensity of phenological dynamics is gathered from different independent measures derived from the NDVI time series (SPOT VEGETATION data from 1998 to 2013).
Where there is a single season, the seasonal integral, an output of the PHENOLO model [10], is used as indicator of the land productivity. It represents the integral of the NDVI between the start and the end of the growing season from which the permanent fraction has been removed. Where there is no or more than one season over the year, the integral (sum) of the NDVI over the year is used instead.
The long-term change of land productivity is characterised by a steadiness index and by the intensity of the change of standing biomass between the beginning and the end of the time series. The steadiness index [11] is a combination of the slope of the linear regression of degree one of the phenological variable on time (year) and the direction of the change between the average of the last three years and all others.

$$MTID3 = \sum_{i=1999}^{2010} \left(\bar{D}_{j \in [2011,2013]} - D_i \right) \tag{2.1}$$

The change in standing biomass is obtained from the differences between the average of the first three years with the last three years. The differences are classified into ten classes and the indicator gives the intensity of the change.
The current status map is obtained by comparing the average performance of the last five years within phenology and productivity related ecosystem functional units (EFUs). Those are determined using five metrics related to the cyclic and permanent fraction of productivity, to the background, to the growing season start and the timing of the maximum NDVI value [10, 12]. The result of the analysis is the relative performance of each pixel with respect to the other pixels within the same EFU, further referred to as local net scaling.
The three datasets are categorised and combined into a global indicator of the direction and intensity of change, as shown in Figure 2.1. Table 2.1 shows how the different levels of the

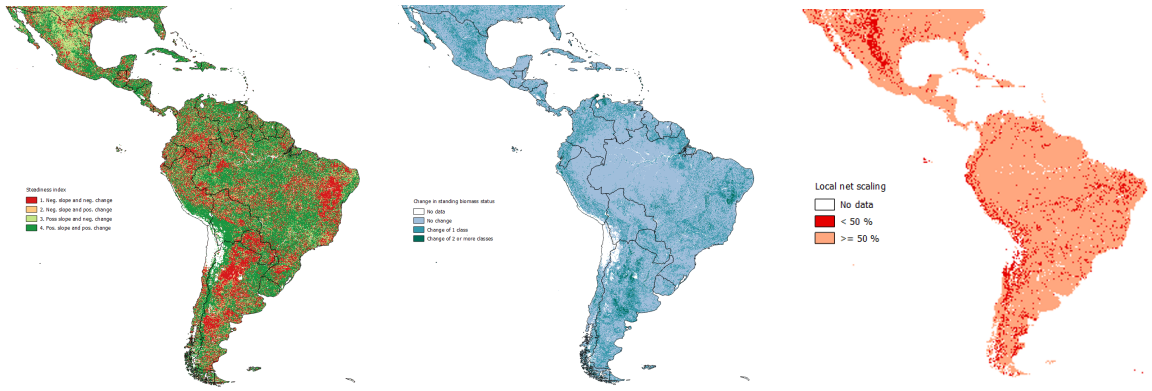

Steadiness index (1999-2013) | Standing biomass state change (99-01 vs 11-13) | Local net scaling (09-13)

Figure 2.1: Combination of weak evidence that converge to give an indicator of the direction and intensity of change in land productivity.

categories are combined into 8 classes. For the interpretation, the 8 classes are merged into 3 classes: evidence of decreasing land productivity, no converging evidence and evidence of increasing land productivity. Figure 2.2 shows the resulting map for Latin America. The red colour indicates the pixels where there is evidence that land productivity is decreasing (values 1 to 3 in table 2.1). The pixels where there is evidence that land productivity is increasing (values 7 to 8) are coloured in green. Between these extremes there is not enough evidence to decide on either increasing or decreasing land productivity. We use the words 'stable land productivity' for these pixels where there is no clear direction in the change.

Table 2.1: Eight classes of convergence of evidence of land productivity dynamics. Low values represent strong evidence of decreasing productivity. High values represent strong evidence of increasing productivity. Middle values express a lack of or contradictory evidence of change.

Steadiness	St1			St2 or St3	St4		
	⇓			?	⇑		
Biomass change	0	1	≥ 2	0 OR 1 OR ≥ 2	0	1	≥ 2
Combined	? ↓	⇓	⇓⇓	?	?↑	⇑	⇑⇑
Local Net Scaling							
$< 50\%$: ↓	⇓	⇓⇓	⇓⇓	↓	?	↑	⇑
	3	2	1	4	5	6	7
$\geq 50\%$: ?	↓	⇓	⇓	?	↑	⇑	⇑⇑
	4	3	3	5	6	7	8

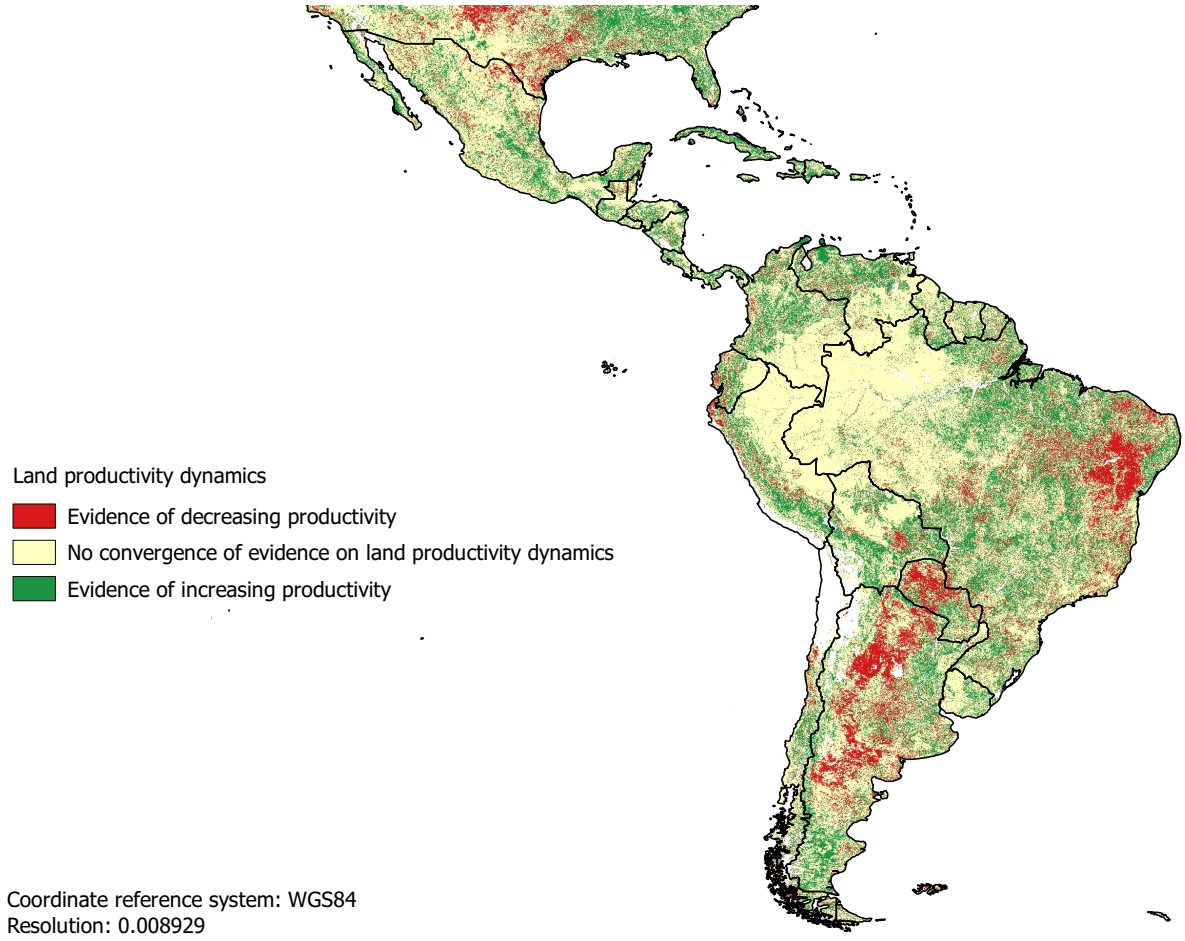

Figure 2.2: Map of the land productivity dynamics

2.2 On the development of combined indicators

Building combined indicators is a delicate task. The combination of single indicators can be compensatory or non compensatory. In the first case, the increase in one of the constituent indicators can be compensated by the decrease of another. The effects can be additive or multiplicative. All kinds of averages, arithmetic or geometric are examples of such compensatory indicators. In the second case, the combined indicators have non-compensatory effects.
Building a non compensatory indicator can be done with methods of data envelopment analysis (DEA), which aim at extracting from the data the "envelopment frontier" where the indicator should be at its maximum. Then, all the observations that are inside the envelope are receiving their indicator's value by projecting the point on the frontier and taking the ratio of the distance from the origin to the observation and the distance from the origin to the projection of the observation on the frontier.
A pure output DEA model is a model where all effects are positive and must be maximised. A single constant input must be considered to make it meaningful [13]. If all output variables are $\in [0, 1]$ and can theoretically take any value in that interval, the DEA indicator simplifies to the maximum value of the output variables. This is demonstrated for the combination of two indicators.
Let $i \in [0, 1]$ and $f \in [0, 1]$ be observations of variables I and F. If the envelopment frontier is made by the line segments joining the points $(I = 1, F = 0), (I = 1, F = 1), (I = 0, F = 1)$, the

projection of (i, f) on the frontier is (i', f') and we can write:

$$\frac{i}{i'} = \frac{f}{f'}$$

and the relative distance ρ of (i, f) on the frontier is:

$$\rho = \frac{(i, \vec{f})}{(i', \vec{f'})} = \frac{\sqrt{i^2 + f^2}}{\sqrt{i'^2 + f'^2}}$$

Hence, we have:

$$\rho = \begin{cases} \frac{\sqrt{i^2+f^2}}{\sqrt{\left(\frac{i}{f}\right)^2+1}} = f & \text{if } i < f, \text{ hence } i' < 1 \text{ and } f' = 1 \\ \frac{\sqrt{i^2+f^2}}{\sqrt{1+\left(\frac{f}{i}\right)^2}} = i & \text{if } i > f, \text{ hence } i' = 1 \text{ and } f' < 1 \\ i = f & \text{if } i = f \end{cases}$$

Which is equivalent to:

$$\rho = \max(i, f)$$

2.3 Human-environment interactions

In this study, we look at human-environment interactions occurring in four classes of land cover (crop, range, forest, urban) that could constitute favourable grounds for land degradation. These are not exclusive and additional information could be taken into account when available at global scale. For each class, we make a distinction between static and dynamic information. Conditions that are prevailing over time are considered as static while ongoing processes involving land cover change are considered as dynamic.
For all variables considered in this study, we create comparable indicators that can take values between 0 and 1. The references of all datasets used in this study are given in table 2.5, page 25.

Table 2.2: IGBP land cover classes (source: NASA LP DAAC at the USGS EROS Center)

Class	IGBP (Type 1)	Class	IGBP (Type 1)
0	Water		
1	Evergreen Needleleaf forest	10	Grasslands
2	Evergreen Broadleaf forest	11	Permanent wetlands
3	Deciduous Needleleaf forest	12	Croplands
4	Deciduous Broadleaf forest	13	Urban and built-up
5	Mixed forest	14	Cropland/Natural vegetation mosaic
6	Closed shrublands	15	Snow and ice
7	Open shrublands	16	Barren or sparsely vegetated
8	Woody savannas	254	Unclassified
9	Savannas	255	Fill Value

2.3.1 Crop land

The expansion of crop land is used as dynamic indicator. We consider two static indicators of susceptibility of crop land to degradation: the intensity of agriculture and the natural constraints to agriculture.

Crop land expansion

The expansion of agricultural land is considered here as likely loss of ecosystem services, although when managed sustainably land can provide greater services than before its conversion.
Land cover change is difficult to evaluate because the uncertainties in land cover classification are large. When comparing land cover maps obtained with the same method for different years, the errors cumulate.
We use the MODIS MCD12Q1 product that gives the global land cover for the years 2001 to 2012, which match our time window (NDVI timeseries: 1999-2013).
Taking the mode of the first and last six years in the time series, we compare them and flag as "expansion" those pixels that are crop land or mosaic cropland/natural vegetation (IBGP classification: 12 and 14, see table 2.2) in the second image and that were not so in the first.

$$CropExp = \begin{cases} 1 & \text{if } \begin{cases} \text{mode}(landCover_{[2001,2006]}) \notin (12,14) \\ \text{mode}(landCover_{[2007,2012]}) \in (12,14) \end{cases} \\ 0 & \text{otherwise} \end{cases} \tag{2.2}$$

Figure 2.3 shows the results of the comparison of the two periods.

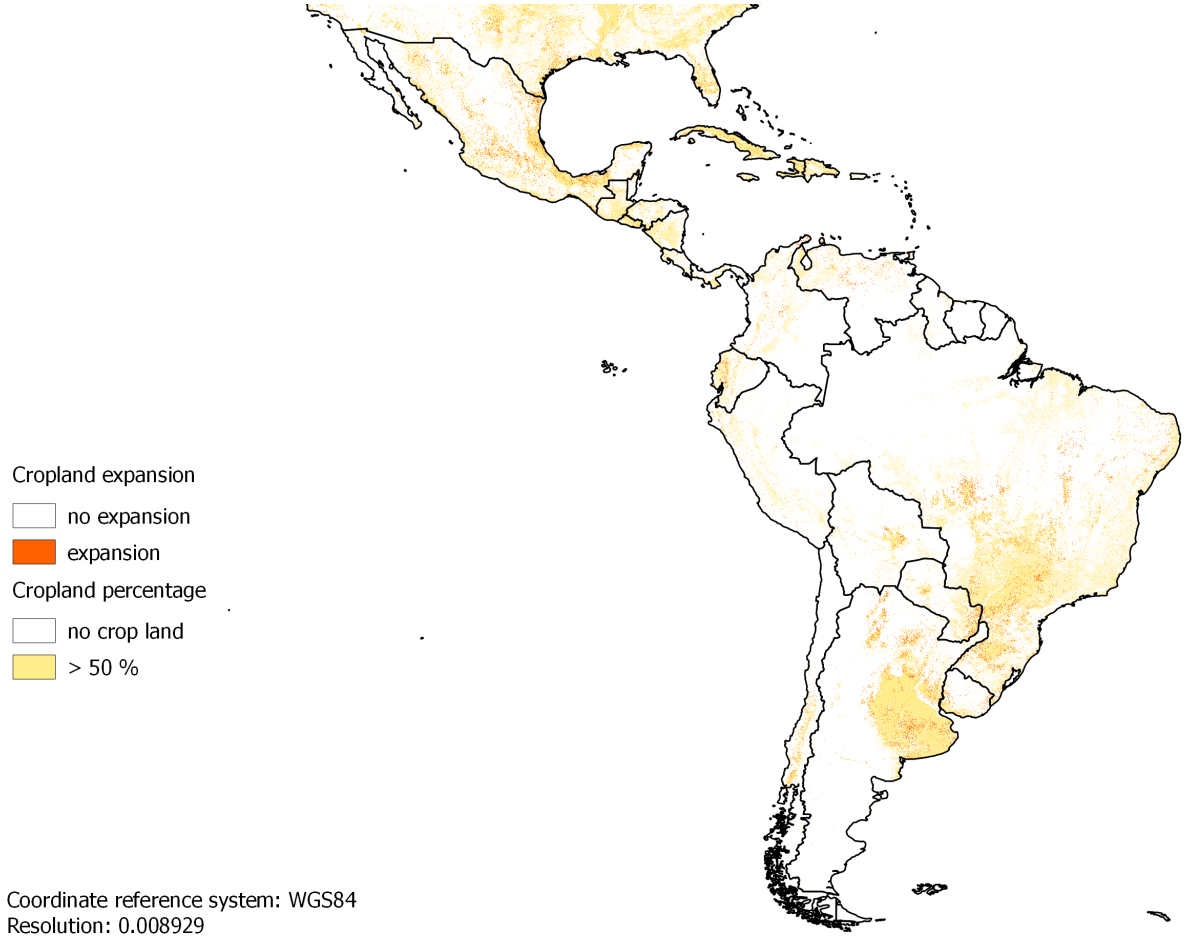

Figure 2.3: Map of crop land expansion in Latin America between the first half and the second half of the observation period.

Agriculture intensity

Intensive agriculture can easily lead to land degradation. Irrigation in regions where water withdrawals are excessive compared to total annual water flow can deplete water resources for the future. Excessive fertilizer application leads to pollution of ground and surface water by infiltration and run-off. Monoculture translates into a loss of ecosystem complexity and often concords with heavy pesticides and fertilizer use.

Irrigation We use the global map of irrigation areas from AQUASTAT that gives the percentage of the area equipped for irrigation. We consider that irrigation constitutes a risk only in regions where water is scarce, that is where the annual withdrawals are large compared to the annual flow of water. We hence use as irrigation indicator the baseline water stress (BWS) in areas equipped for agriculture and clamp it between 0 and 1. This means that a BWS of 1 or more is set to 1, the maximum value. All pixels with a non null percentage of the area equipped for irrigation that have a BWS above 0.5 are flagged.

Fertilization According to the literature, 30 kg/ha are considered as a moderate residual of nitrogen [14]. We clamp the total nitrogen balance on landscape [15] between 0 and 60 kg/ha and divide it by 60 to have an indicator that varies between 0 and 1 and that is centred on a moderate residual of nitrogen.

$$Fertilization = \min\left(\max\left(0, \frac{N}{60}\right), 1\right) \tag{2.3}$$

Monoculture Pixels where at least one of the major crops (i.e. maize, rice, wheat, soybean, sugarcane) [16] covers at least 40 % of the area are flagged as monoculture (1) while the others are assigned a value of 0.

$$Monoculture = \begin{cases} 1 & \text{if any of (maize, rice, wheat, soybean, sugarcane)} > 40\% \\ 0 & \text{otherwise} \end{cases} \tag{2.4}$$

The three indicators of agriculture intensity are combined by taking their maximum.

$$CropIntensity = \max\left(Irrigation, Fertilization, Monoculture\right) \tag{2.5}$$

Figure 2.4 shows the three components of the cropIntensity indicator as RGB, under a cropland mask. Red, green and blue pixels show where a single component is at play, while where two or three components have non null values, the colours are combined. Places where the area under cropland is more than half the surface, but where all three components are null appear in black.

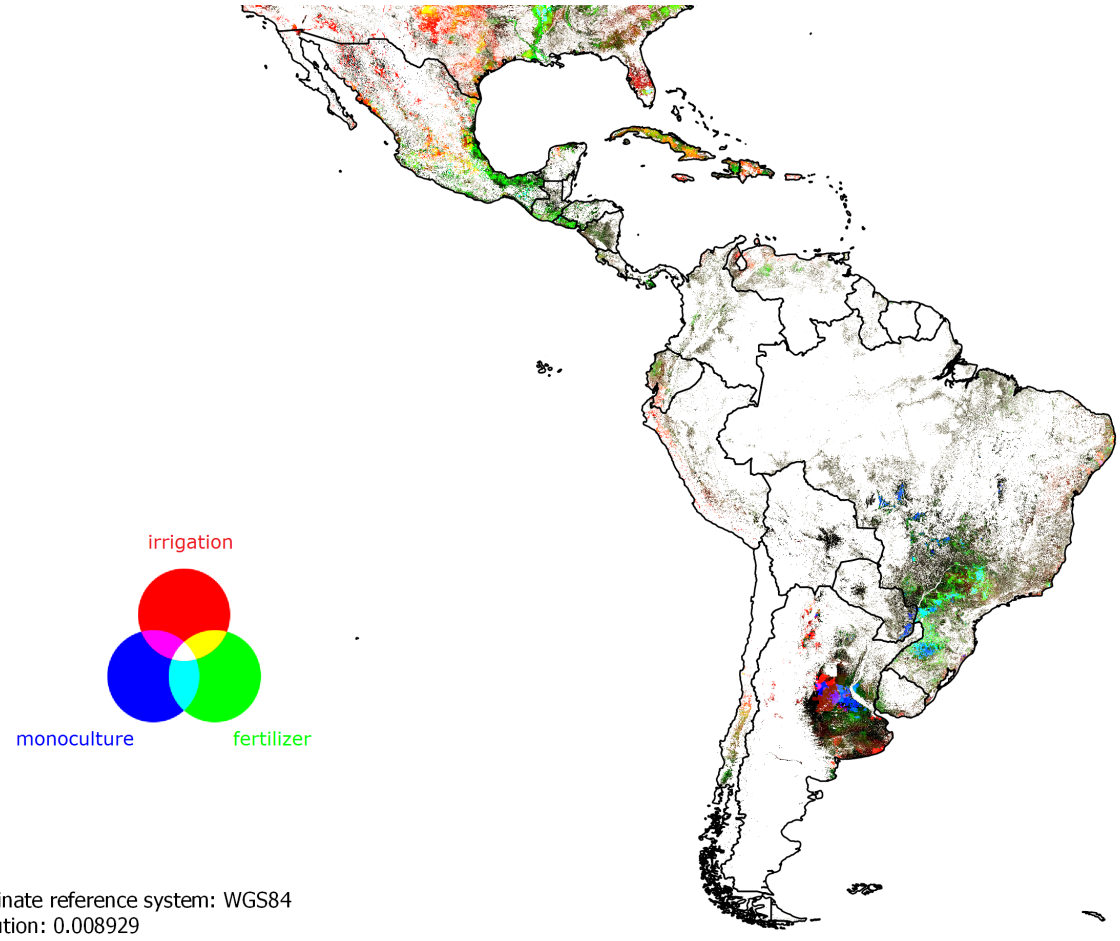

Figure 2.4: Map of agriculture intensity indicator in crop lands of Latin America. Red: Baseline water stress in irrigated areas; Green: Nitrogen residual; Blue: Monoculture. The colours are combined as RGB. Pixels where all three components are null are black.

Constraints to agriculture

Agriculture in constrained areas can have disastrous effects on land if management is not properly adapted. The constraints can be overcome by adapted technologies but constitute a non-negligible vulnerability, especially when they are associated with poverty. Natural constrains can be due to soil quality, terrain and climate.

Soil Poor soil quality can constrain agriculture. We use the FAO/IIASA map of global areas with soil constraints developed on the basis of the FAO/UNESCO Digital Soil Map of the World in the framework of the Global Agro Ecological Zones (GAEZ). The shallower the soil and the poorest his quality, in terms of natural fertility, toxicity, drainage and texture, the more it impedes agriculture. The degree to which soil characteristics constrain agricultural production potential in the pixel area is rated from 1 to 7 [17]. We subtract 1 and divide by 6 to obtain an indicator in the range $[0, 1]$.

Terrain Over 15 degrees of slope, crop production is severely constrained. Terracing or other adaptation is necessary to avoid excessive loss of soil. We use the USGS digital elevation model to derive the slope. We clamp the values between 0 and 15 and divide by 15 to have a indicator ranging between 0 and 1.

Climate When climatic conditions are too dry or too cold, the length of the growing period is too short to allow crop production without irrigation or heated greenhouses. We use maps of the length of moisture and temperature constrained growing period developed for the GAEZ. We consider 150 and 210 days as maximum values for the moisture and temperature growing periods respectively. We build the indicator for climate constraint as follows:

$$ClimConstr = 1 - (\min(\max(mgp, 150), (\max(tgp, 210) - 60))/150) \tag{2.6}$$

where mgp and tgp are the lengths of growing period constrained by moisture and temperature respectively.
The three constraints are combined in a single static indicator by taking their maximum:

$$CropConstr = \max(SoilConstr, SlopeConstr, ClimConstr) \tag{2.7}$$

Similarly to the CropIntensity indicator, Figure 2.5 shows the three components of the indicator of constraints to agriculture as RGB. The two static indicator related to crop land are combined by taking their maximum:

$$CropInd = \max(CropIntensity, CropConstr) \tag{2.8}$$

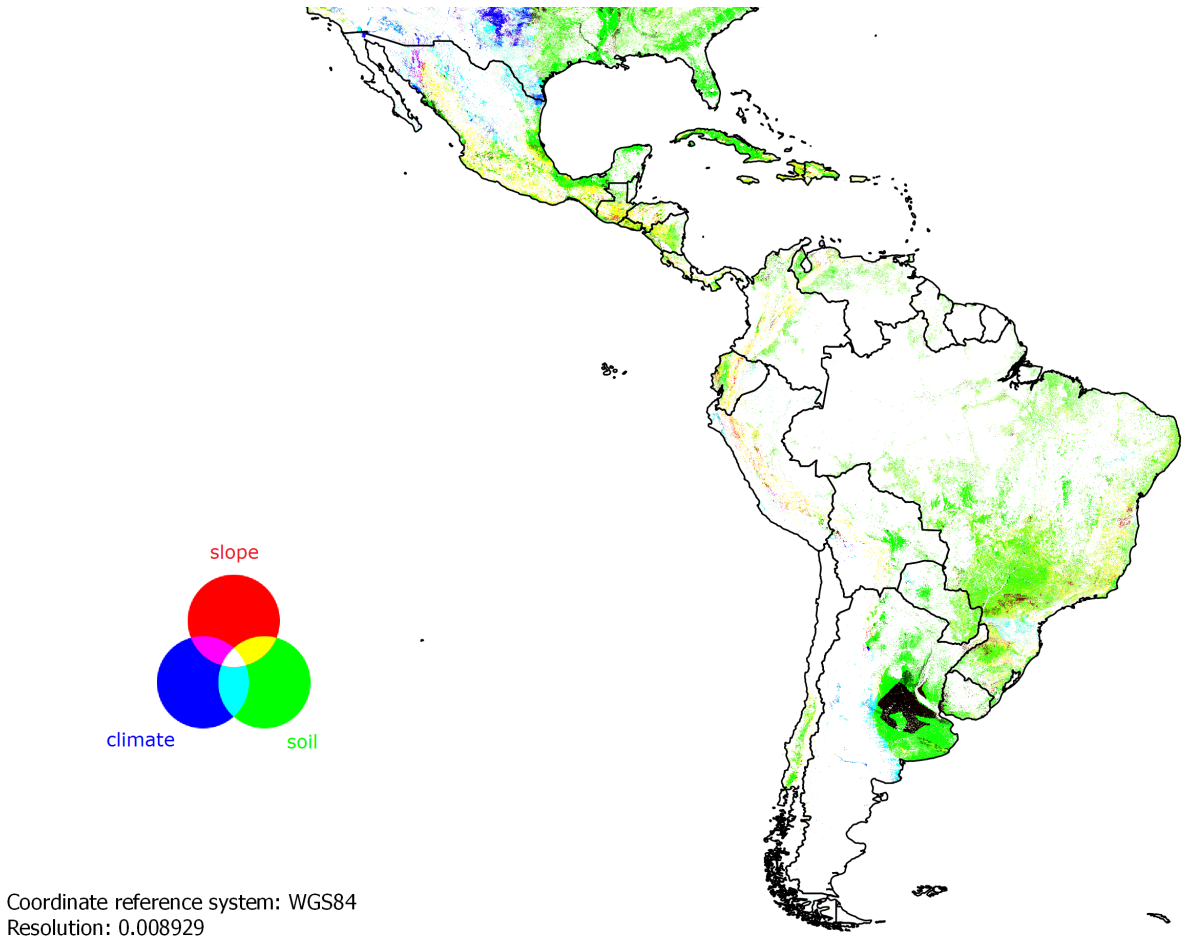

Figure 2.5: Map of constraints to agriculture in crop lands of Latin America. Red: slope; Green: soil; Blue: climate. The colours are combined as RGB. Where all three components are null, colour is black.

2.3.2 Range land

In range land, the land use change is difficult to assess given the large number of land cover classes that it can encompass. As range land mask, we use the IGBP classes 6 to 11 as well as 14 and 16 (Table 2.2).
We assess the intensity of animal husbandry with livestock density. We build two indicators of intensity: one related to the feeding capacity of the land and the other with the risk of nitrogen pollution.
We could not assess the expansion of the range lands themselves nor issues such as bush encroachment or presence of invasive alien species at global scale.

Livestock density

High stocking rates do not allow the grass to regrow and may lead to land degradation through loss of biological productivity or bush encroachment. We use the modelled livestock density from FAO, with the livestock unit (LSU) coefficients from EUROSTAT (Table 2.3) and the median yearly net primary production from NASA to build an indicator of the pressure of the stocking rate of grazers on the range lands. The LSU is a reference unit established initially on the basis of the nutritional or feed requirement of each type of animal. One LSU is the grazing equivalent of one adult dairy cow producing 3000 kg of milk annually. We convert all livestock densities in LSU by multiplying them by the corresponding LSU coefficient and add the layers to obtain a unique livestock density layer.

Table 2.3: Livestock unit coefficients and recommended number of animals per square kilometre

Animal type	LSU	# /km^2
Cattle/beef	0.8	63
Pigs	0.5	125
Sheep/Goats	0.15	500
Poultry	0.014	5000

$$GrazerDensity = (cattle * 0.8 + sheep * 0.15 + goats * 0.15) \tag{2.9}$$

Stocking rate

We compute the maximum stocking rate that can be supported as a function of the net primary productivity (NPP) based on the following assumptions:

- The above ground biomass accounts for half of the total NPP [kg of C per square km per year]
- According to the "take half, leave half" method, the available forage for grazers is about half of the above ground biomass [18].
- The daily metabolic requirement of a cow with calf (reference for 1 LSU) ranges from 1 to 2.8 % of its body weight [19]. We used 2.667% of 450 kg, i.e. 12 kg of dry matter [18].
- One kg of dry matter contains 0.475 kg of carbon

$$availableForage = 0.5 * 0.5 * \text{median}(NPP_{2000,2013}) \tag{2.10a}$$
$$animalIntake = 12 * 0.475 * 365 \tag{2.10b}$$
$$maxStockingRate = \frac{availableForage}{animalIntake} \tag{2.10c}$$

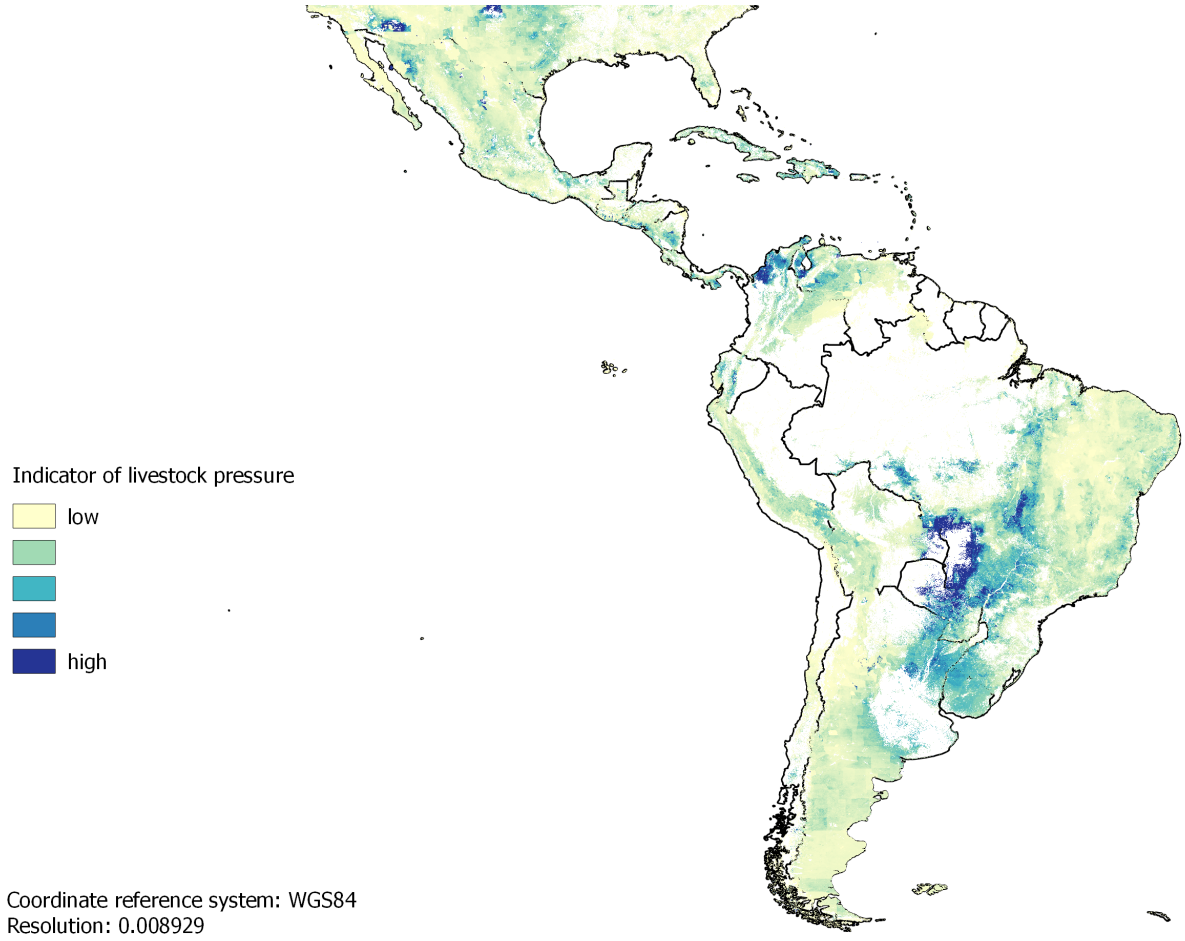

Figure 2.6: Map of indicator of pressure exerted by grazers on range lands of Latin America.

We build an indicator of the intensity of the stocking rate by taking the ratio of the grazer density and the maximum stocking rate that can be supported. Where the indicator is below 1, the grazer density can be supported by the local productivity. Where it is above one, the grazer density is too large for the local productivity and the vegetation cannot recover without additional input (fertilizer or concentrated feedstuffs). We divide the indicator by 2 and clamp it between 0 and 1 to make it comparable with the other indicators.

$$grazerIntensity = \min\left(\frac{grazerDensity}{2 * maxStockingDensity}, 1\right) \tag{2.11}$$

Figure 2.6 shows the resulting indicator. The darker the shade, the greater the pressure on the land. The calculation is greatly simplifying the real situation since it does not consider the seasonal variations. The indicator is hence probably too optimistic.

Risk of nitrate leaching

The EU Nitrates Directive sets the limit of 170 kg/ha/year as maximum nitrogen input from agricultural sources [20]. In livestock raising, this translates into about 240 LSU/km^2/year. The indicator of nitrogen production is hence the minimum between the annual livestock density divided by twice the maximum allowed input and one. Figure 2.7 shows the spatial distribution

Figure 2.7: Map of indicator of livestock nitrogen production on range lands of Latin America.

of the indicator in Latin America.

$$livestockDensity = (0.8cattle + 0.15sheep + 0.15goats + 0.5pigs + 0.014poultry) \tag{2.12a}$$

$$NleachingRisk = \min\left(\frac{livestockDensity}{240 * 2}, 1\right) \tag{2.12b}$$

Both indicators can be combined by taking their maximum.

$$RangeInd = \max\left(grazerIntensity, NleachingRisk\right) \tag{2.13}$$

2.3.3 Forest

We consider deforestation as direct loss of ecosystem services, through loss of ecosystem complexity, biological production and economic production. As dynamic indicator, we use the Hansen Global Forest Change v1.1 that assesses tree loss from 2000 to 2013 as shown in Figure 2.8.

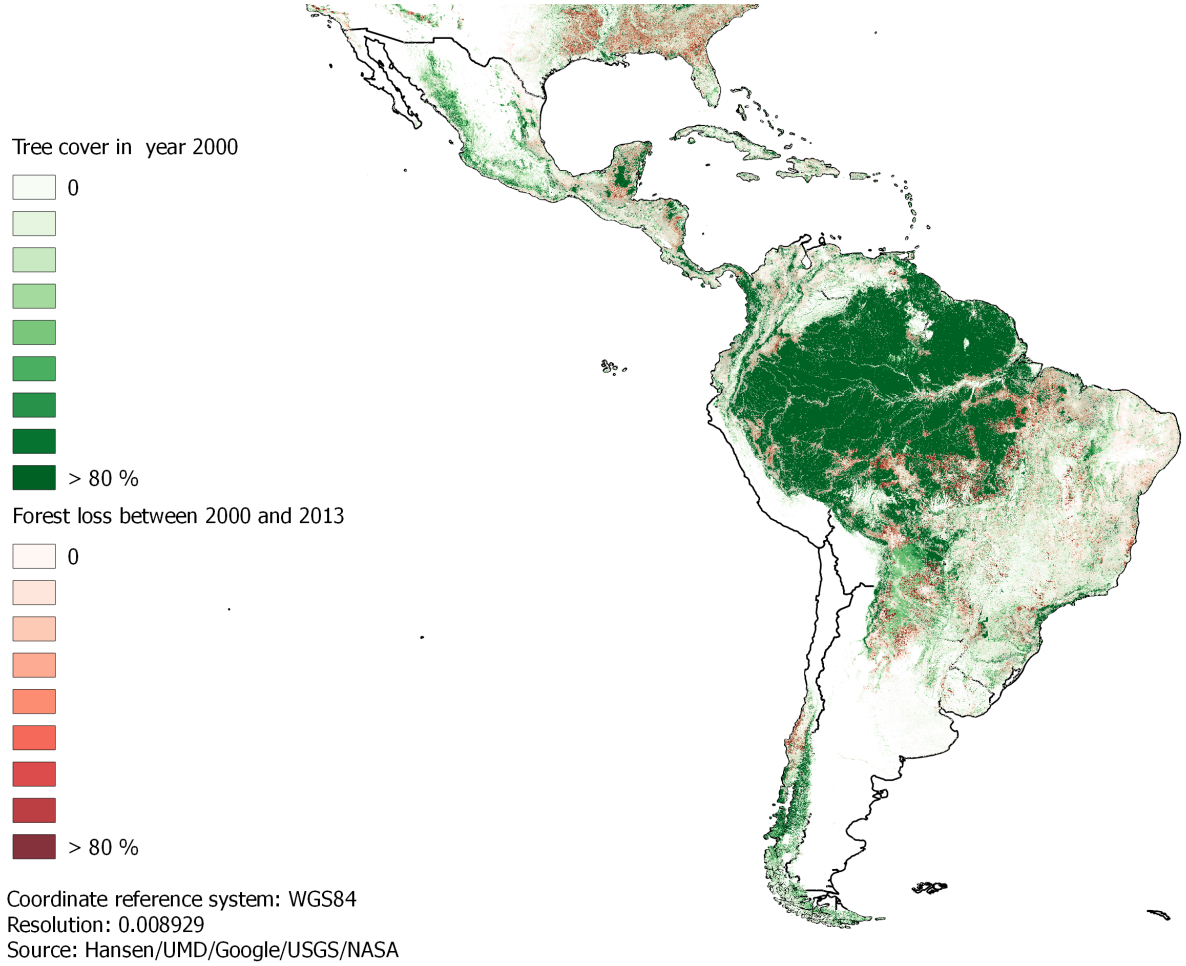

Figure 2.8: Map of indicator of forest loss in Latin America.

2.3.4 Urban

The expansion of urbanized areas results in soil sealing and loss of other ecosystem services that the land could provide. We use the Global Human Settlement Layer [21] to assess the expansion of settlements and soil sealing between 2000 and 2014 (Figure 2.9).

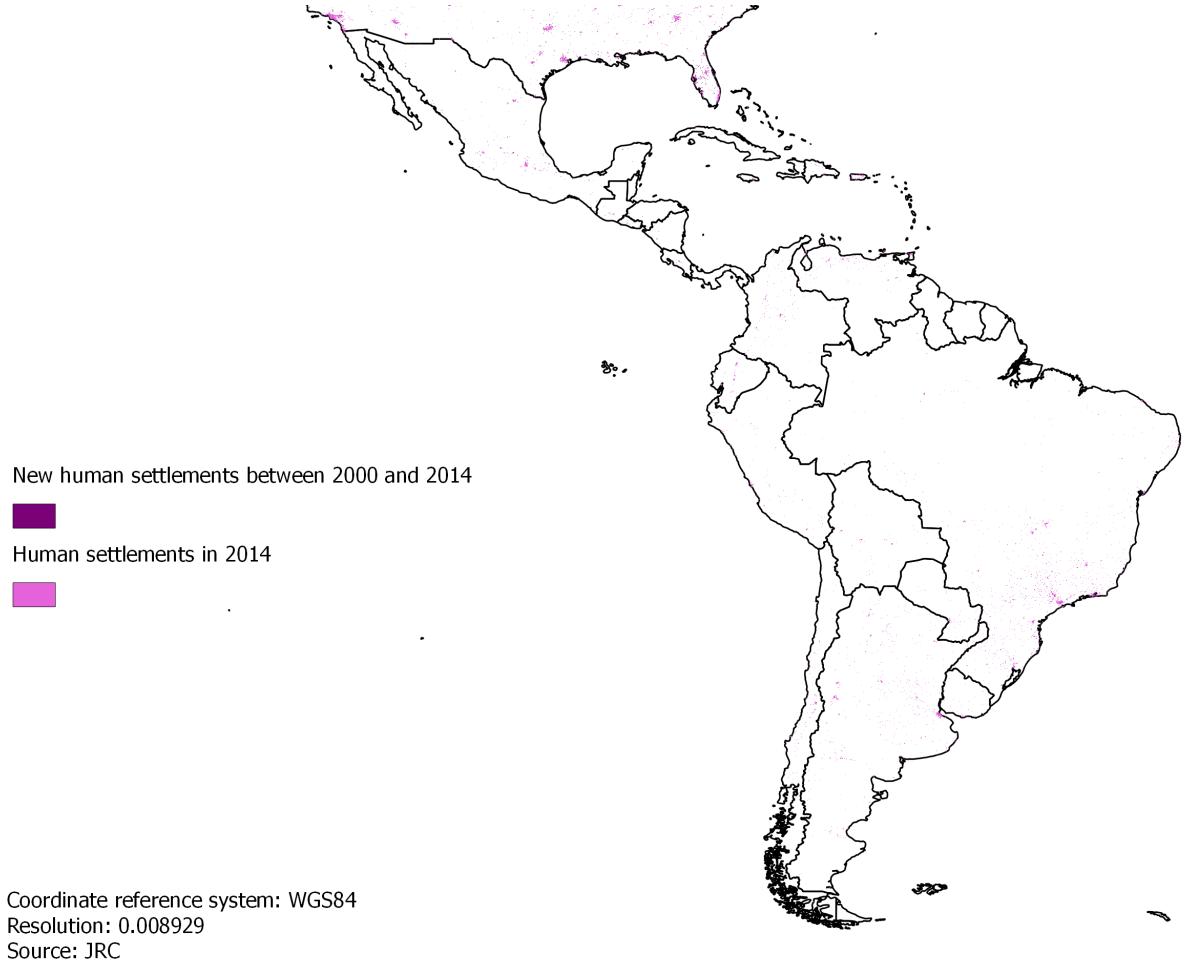

Figure 2.9: Map of human settlements in Latin America.

2.3.5 Overarching factors

We selected additional layers that are not related with any particular land use but can aggravate the conditions that could lead to land degradation.

Fire

Wildfires represent an important agent of land degradation in temperate sub humid ecosystems [22]. These are different than prescribed fires. They remove the vegetation and make the soil more susceptible to wind/water erosion. For example in Mediterranean countries, the frequency of wild fires increases due to the migration of the rural population and the land abandonment. The post-fire erosion rate decreases after several months or years: the window of disturbance is generally limited in time.
In this study we use the burning occurrence based on the analysis of MODIS AQUA/TERRA data between 1999 and 2013. The data are shown in Figure 2.10.

Drought

Areas that have been hit by more severe drought events than one could expect are likely to exhibit a decrease in land productivity. Droughts can have an effect on land similar to wildfires, with an increased susceptibility to erosion. Long lasting droughts can lead to land degradation when the vegetation cannot recover and the land cannot reach its former productivity.
The Standardized Precipitation Index (SPI) is a statistical indicator used for comparing the

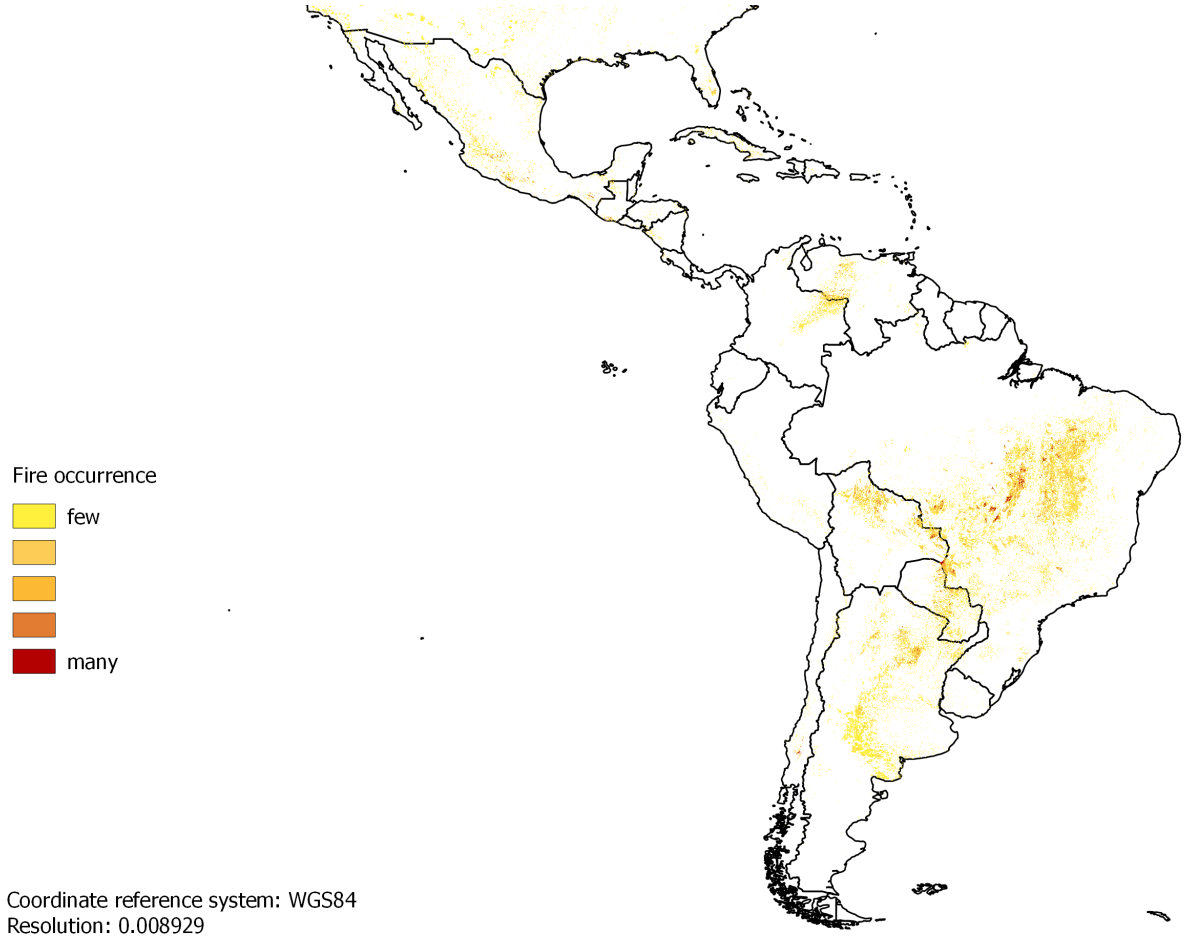

Figure 2.10: Map of fire occurrence between 1999 and 2013 in Latin America.

precipitation at a certain location with the long-term distribution of rainfall at the same location. It is calculated monthly for a cumulation period of n months. The distribution is normalised to allow the comparison of different climates. The magnitude of departure from the mean is a probabilistic measure of the severity of a wet or dry event (Table 2.4). We use the SPI-12 calibrated on the reference period 1981-2010 computed with data from the Global Precipitation Climatology Centre (GPCC), available from the JRC drought observatory [23]. The total number of months in our observation period (1999-2013) is 180. By comparing the number of months in a given class of SPI during that period with the theoretical probability multiplied by 180 (table 2.4), we can highlight the locations that underwent more extreme drought events than one could expect. Figure 2.11 shows anomalies that correspond to well defined events during that period: extreme drought in north-east Brazil from 2012 to today; Amazonia in 2005 and 2010; Argentina in 1998/1999 and 2011/2012.

Table 2.4: Standardized Precipitation Index (SPI) classification [24]

SPI	Class	Probability of event [%]
$\text{SPI} \geq 2.00$	Extreme wet	2.3 %
$1.50 < \text{SPI} \leq 2.00$	Severe wet	4.4 %
$1.00 < \text{SPI} \leq 1.50$	Moderate wet	9.2 %
$-1.00 < \text{SPI} \leq 1.00$	Near normal	68.2 %
$-1.50 < \text{SPI} \leq -1.00$	Moderate dry	9.2 %
$-2.00 < \text{SPI} \leq -1.50$	Severe dry	4.4 %
$\text{SPI} < 2.00$	Extreme dry	2.3 %

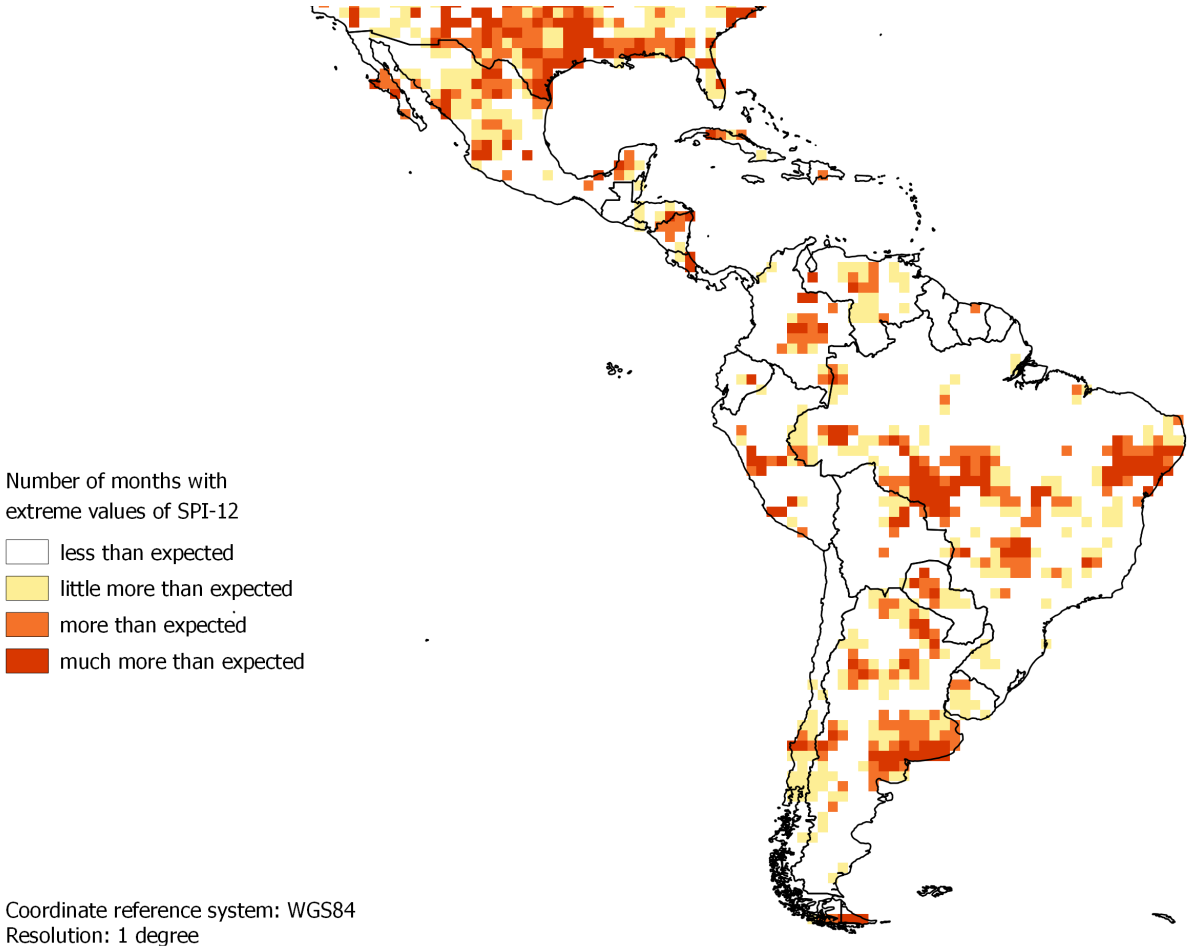

Figure 2.11: Map of the number of months with SPI-12 values corresponding to severe droughts in the period 1999 to 2013 in Latin America.

Poverty

The relation between poverty and land degradation is one of negative feedback [25]. In areas of desertification there is a great incidence of poverty and indigence. Poverty and indigence affect rural populations in greater proportion, even if there are more poor in cities (just because urban population is larger than rural). Drought and desertification favour poverty and the breaking of family structures.
Rural poverty statistics can be incorporated in the analysis, but are difficult to obtain at subnational levels, which makes their relevance disputable in this context. Also, those statistics do not consider the informal sector of the economy. For example, smallholder farmers who practice subsistence agriculture using viable, sustainable practices with good resilience to environmental risks could have little monetary income but still meet their needs and have no adverse effect on the land they care for. Given the former shortcomings, we did not include poverty statistics in the analysis.

2.4 Combined indicator of susceptibility to land degradation

We consider the susceptibility to land degradation as the maximum of all previous indicators:

$$ldd = \max\left(CropExp, CropInd, RangeInd, TreeLoss, UrbanExp\right) \tag{2.14}$$

Table 2.5: List of spatial layers integrated in the analysis

Indicator	Layer Name	Time frame	Resolution [degree] (km)	Provider
Crop land	Cropland Map	2005	0.0083 (1 km)	IIASA-IFPRI [26]
Agriculture expansion	MCD12Q1	2001-2012	0.5 km	NASA LP DAAC at the USGS EROS Center [27]
Agriculture intensity				
Irrigation	Global Map of Irrigation Areas v5.0	2013	0.083 (10 km)	AQUASTAT-Universität Bonn [28]
Water scarcity	Aqueduct Global Maps 2.1 Data: Baseline Water Stress	2010		WRI AQUEDUCT [29]
Fertilization	Total Nitrogen Balance for 140 Crops	2000	0.083 (10 km)	EarthStat/GLI [15]
Monoculture	Harvested areas of major crops	2000	0.083 (10 km)	EarthStat [16]
Constraints to agriculture				
Soil quality	Global areas with soil constraints	-	0.083 (10 km)	FAO-IIASA [17]
Terrain	Global Multi-resolution Terrain Elevation Data	2010	0.002 (0.23 km)	USGS [30]
Climate	Length of growing period	1950-2000	0.083 (10 km)	GAEZ-FAO-IIASA [31]
Range land				
Livestock density	Modelled livestock density	2006	0.0083 (1 km)	FAO-ILRI-ERGO-ULB [32]
Net primary production	MOD17A3H.006	2000-2015	0.0042 (500 m)	NASA LP DAAC at the USGS EROS Center [33]
Forest loss	Hansen Global Forest Change v1.1	2000-2013	(30 m)	Hansen-UMD-Google-USGS-NASA [34]
Urban expansion	Global Human Settlement Layers	1975-2014	(38 m)	JRC
Drought severity	SPI-12	1999-2013	1 (110 km)	JRC drought observatory [23]
Fire occurrence	MCD45A1	2000-2013	0.00833 (1 km)	NASA LP DAAC at the USGS EROS Center [35]

3 Interpretation of human-environment interactions

Where the land productivity dynamics map indicate a decreasing productivity and the susceptibility to land degradation has values larger than 0.5, there is convergence of evidence that land degradation is likely to occur. However increasing productivity can disguise degradation processes, for example due to unsustainable practices under intensive agriculture that are depleting the water resources or causing pollution. Also, decreasing productivity may be caused by short lasting processes that won't induce permanent loss of ecosystem services, but from which the land can recover by itself after a few years if managed properly. It may be the case of certain fire and drought events.

Figure 3.1 shows the results of this interpretation over Latin America based on the land productivity dynamics shown at Figure 2.2.

The red colour shows all pixels with decreasing land productivity where the combined indicator of susceptibility to land degradation is larger than 0.5. This does not show which particular indicator contributed to the interpretation nor under what land use it is. For further information, the values of the individual indicators are distributed in another raster file, which is accessible on the scado portal (http://edo.jrc.ec.europa.eu/scado/) and as a Google Earth Engine asset (users/mweynants/WAD/LDSusceptibilityIndic).

The orange colour shows the pixels that are classified as having increasing land productivity where the indicator for intensive agriculture is greater than 0.5 and where more than 50% of the area is dedicated to crops. The yellow colour shows the same for pixels that are classified as stable productivity. Both indicate areas where agriculture practices are potentially unsustainable, which could lead to the degradation of the resources, e.g. depletion of the water table due to overexploitation of water, pollution due to excess use of fertilizers, loss of biodiversity due to monoculture.

The brown pixels show areas where the ruminant stocks are greater than those that can be supported by the natural vegetation but where there is no sign of a decline in land productivity. This could indicate that the livestock is fed supplementary feed. It could also indicate a risk of overexploitation of the land resource that might lead to bush encroachment or other loss of biodiversity.

The light blue colour indicates areas where there is evidence that the land productivity has decreased that suffered more extreme droughts than expected or where fires occurred during the observation period. This could mean that the land might recover a stable or increasing productivity in the future. In the meantime, the soil is more susceptible to erosion and degradation may occur. Furthermore, in case of long-lasting extreme droughts or frequent fires, the soil may degrade heavily and the land may not be able to recover its previous productivity.

The remaining colours show the areas where none of the indicators considered here indicates a particular pattern of land degradation. The last entry in the legend has been added because the confidence in the land productivity change in mountainous areas (defined as elevation greater than 1000 m or slope steeper than 30 degrees) is less than in flatter areas.

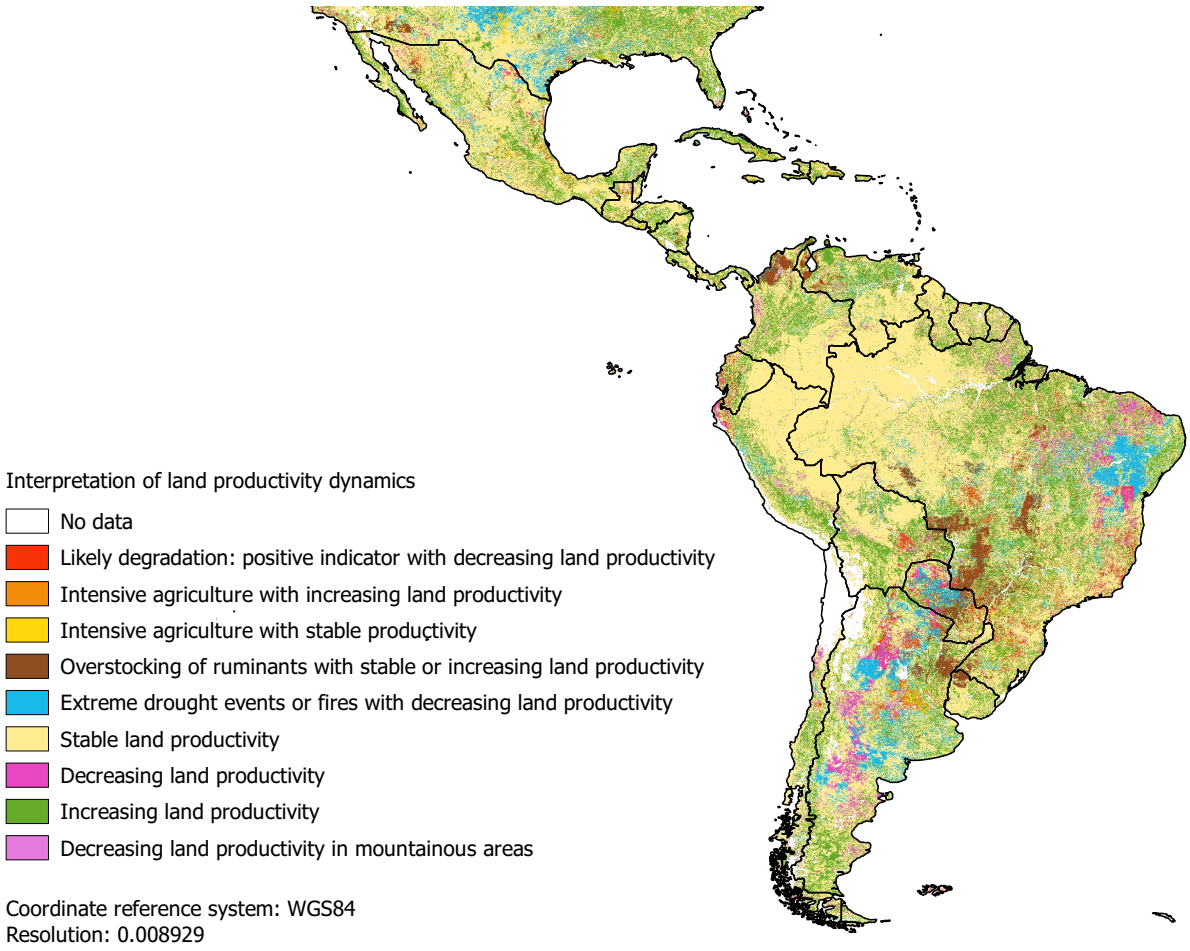

Figure 3.1: Map of the interpretation of the land productivity dynamics based on the indicators of human-environment interactions

4 Conclusions and perspectives

The monitoring of land degradation processes is of main importance to understand the areas that are at risk, and keep them monitored in time will help to evaluate if the measures taken are being effective in combating desertification and land degradation. Land degradation is not a unique process that can be mapped with a single indicator at global scale. It is rather a combination of processes acting conjointly that can have additive effects. In this study, we suggest an approach to interpret bio-physical data, here the land productivity dynamics, using indicators of human-environment interactions.

The results are maps that highlight areas where societal and environmental conditions have changed in the last 15 years and that require closer scrutiny. They are not land degradation maps as such because it cannot be apprehended with the data available at continental or global scale. Further detailed investigation is needed to determine whether land degradation is indeed occurring and what should be done to halt it. The top-down approach used here needs to be confirmed by the bottom-up perspective. Besides, the current analysis could be improved by adding socio-economical data. Unfortunately, these are not currently available throughout the region at subnational level. They could however be included in future case-studies.

We draw attention to the limitation of data availability at global or continental scale. The resolution and quality of the different datasets we used is uneven and can cause inconsistencies in the final integration. However, the methodology presented here can easily be adapted to incorporate new better datasets when they become available. The script of the analysis is available on Google Earth Engine (GEE) at https://code.earthengine.google.com/2788dacdb114820898bd7a8c94a4788e and the interpretation and indicators maps can be imported in new GEE scripts using image IDs "users/mweynants/WAD/lpdInterp" and "users/mweynants/WAD/LDSusceptibilityIndic" respectively.

Bibliography

[1] FAO, Natural Resources and Environment: Land Degradation Assessment.
URL http://www.fao.org/nr/land/degradation/en/

[2] Millennium Ecosystem Assessment, Ecosystems and Human Well-being: Synthesis, Island Press, Washington, DC, 2005.

[3] K. Rasmussen, D. Sarah, R. Fensholt, Environmental change in the Sahel : reconciling contrasting evidence and interpretations, Regional Environmental Change 16 (2016) 673–680. doi:10.1007/s10113-015-0778-1.

[4] T. Caspari, G. van Lynden, Z. Bai, Land Degradation Neutrality: An Evaluation of Methods, Tech. rep., Series: Texte 62/2015, Dessau-Rosslau.
URL http://www.umwelbundesamt.de/publikationen/land-degradation-neutrality-an-evaluation-of

[5] ISRIC, GLASOD.
URL http://www.isric.org/projects/global-assessment-human-induced-soil-degradation-glasod

[6] F. O. Nachtergaele, M. Petri, R. Biancalani, G. van Lynden, H. van Vethuizen, M. Bloise, Global Land Degradation Information System (GLADIS) version 1.0. An information database for land degradation assessment at global level, Tech. Rep. September, LADA (2011).

[7] H. Gibbs, J. Salmon, Mapping the world's degraded lands, Applied Geography 57 (2015) 12–21. doi:10.1016/j.apgeog.2014.11.024.

[8] Z. G. Bai, D. L. Dent, L. Olsson, M. E. Schaepman, Proxy global assessment of land degradation, Soil Use and Management 24 (3) (2008) 223–234. doi:10.1111/j.1475-2743.2008.00169.x.

[9] P. Brabant, C. Cheverry, Dégradation mondiale des terres : comment l'évaluer ? - Les Mots de l'agronomie (Jul. 2012).
URL http://mots-agronomie.inra.fr/mots-agronomie.fr/index.php/D%C3%A9gradation_mondiale_des_terres_:_comment_l%27%C3%A9valuer_%3F

[10] E. Ivits, M. Cherlet, W. Mehl, S. Sommer, Ecosystem functional units characterized by satellite observed phenology and productivity gradients: A case study for Europe, Ecological Indicators 27 (2013) 17–28. doi:10.1016/j.ecolind.2012.11.010.

[11] E. Ivits, M. Cherlet, S. Sommer, W. Mehl, Addressing the complexity in non-linear evolution of vegetation phenological change with time-series of remote sensing images, Ecological Indicators 26 (2013) 49–60. doi:10.1016/j.ecolind.2012.10.012.

[12] E. Ivits, M. Cherlet, S. Horion, R. Fensholt, Global biogeographical pattern of ecosystem functional types derived from earth observation data, Remote Sensing 5 (7) (2013) 3305–3330. doi:10.3390/rs5073305.

[13] C. Lovell, J. T. Pastor, Radial DEA models without inputs or without outputs, European Journal of Operational Research 118 (1) (1999) 46–51.

[14] A. Shrestha, Cropping systems: trends and advances, CRC Press, 2004.

[15] P. C. West, J. S. Gerber, P. M. Engstrom, N. D. Mueller, K. a. Brauman, K. M. Carlson, E. S. Cassidy, M. Johnston, G. K. MacDonald, D. K. Ray, S. Siebert, Leverage points for improving global food security and the environment, Science 345 (6194) (2014) 325–328. doi:10.1126/science.1246067.

[16] C. Monfreda, N. Ramankutty, J. a. Foley, Farming the planet: 2. Geographic distribution of crop areas, yields, physiological types, and net primary production in the year 2000, Global Biogeochemical Cycles 22 (1) (2008) 1–19. doi:10.1029/2007GB002947.

[17] H. van Velthuizen, B. Huddleston, G. Fischer, M. Salvatore, E. Ataman, F. O. Nachtergaele, M. Zanetti, M. Bloise, A. Antonicelli, J. Bel, A. de Liddo, P. de Salvo, G. Franceschini, Mapping biophysical factors that influence agricultural production and rural vulnerability, FAO/IIASA, Rome, 2007.

[18] M. Pratt, G. Allen Rasmussen, Determining Your Stocking Rate, Tech. rep., Utah State University Extension (2001).
URL http://digitalcommons.usu.edu/extension_histall/993

[19] F. J. Cordova, J. D. Wallace, R. D. Pieper, Forage Intake by Grazing Livestock: A Review, Journal of Range Management 31 (November).
URL https://journals.uair.arizona.edu/index.php/jrm/article/view/6880/6490

[20] Council of the European Communities, Council Directive of 12 December 1991 concerning the protection of waters against pollution caused by nitrates from agricultural sources (1991).
URL http://data.europa.eu/eli/dir/1991/676/oj

[21] M. Pesaresi, Guo Huadong, X. Blaes, D. Ehrlich, S. Ferri, L. Gueguen, M. Halkia, M. Kauffmann, T. Kemper, Linlin Lu, M. A. Marin-Herrera, G. K. Ouzounis, M. Scavazzon, P. Soille, V. Syrris, L. Zanchetta, A Global Human Settlement Layer From Optical HR/VHR RS Data: Concept and First Results, IEEE Journal of Selected Topics in Applied Earth Observations and Remote Sensing 6 (5) (2013) 2102–2131. doi:10.1109/JSTARS.2013.2271445.

[22] T. C. J. Esteves, M. J. Kirkby, R. a. Shakesby, a. J. D. Ferreira, J. a. a. Soares, B. J. Irvine, C. S. S. Ferreira, C. O. a. Coelho, C. P. M. Bento, M. a. Carreiras, Mitigating land degradation caused by wildfire: Application of the PESERA model to fire-affected sites in central Portugal, Geoderma 191 (2012) 40–50. doi:10.1016/j.geoderma.2012.01.001.

[23] European Commission Joint Research Centre, Global Drought Observatory (2016).
URL http://edo.jrc.ec.europa.eu/gdo

[24] T. B. McKee, J. Nolan, J. Kleist, The relationship of drought frequency and duration to time scales, in: Preprints, Eighth Conf. on Applied Climatology, Anaheim, CA, Amer. Meteor, Soc., 1993, pp. 179–184.

[25] C. Morales, S. Parada (Eds.), Pobreza, desertificación y degradación de los recursos naturales, Naciones Unidas, Santiago de Chile, 2005.

[26] S. Fritz, L. See, I. a. N. Mccallum, L. You, A. Bun, E. Moltchanova, M. Duerauer, F. Albrecht, C. Schill, C. Perger, P. Havlik, A. Mosnier, P. Thornton, U. Wood-sichra, M. Herrero, I. Becker, Mapping global cropland and field size, Global Change Biology 21 (2015) 1980–1992. doi:10.1111/gcb.12838.

[27] M. A. Friedl, D. Sulla-menashe, B. Tan, A. Schneider, N. Ramankutty, A. Sibley, X. Huang, MODIS Collection 5 global land cover : Algorithm refinements and characterization of new datasets, Remote Sensing of Environment 114 (1) (2010) 168–182. doi:10.1016/j.rse.2009.08.016.

[28] S. Siebert, V. Henrich, K. Frenken, J. Burke, Global Map of Irrigation Areas version 5. (2013).
URL http://www.fao.org/nr/water/aquastat/irrigationmap/

[29] F. Gassert, M. Luck, M. Landis, P. Reig, T. Shiao, AQUEDUCT Global Maps 2.1 : Constructiong Decision-RelevantGlobal Water Risk Indicators (2015).
URL http://www.wri.org/publication/aqueduct-global-maps-21-indicators

[30] J. Danielson, D. Gesch, Global multi-resolution terrain elevation data 2010 (GMTED2010) (2011).

[31] IIASA/FAO, Global Agro-ecological Zones (GAEZ 3.0) (2012).

[32] T. P. Robinson, G. R. W. Wint, G. Conchedda, T. P. Van Boeckel, V. Ercoli, E. Palamara, G. Cinardi, L. D'Aietti, S. I. Hay, M. Gilbert, Mapping the global distribution of livestock., PloS one 9 (5) (2014) e96084. doi:10.1371/journal.pone.0096084.

[33] S. Running, Q. Mu, M. Zhao, MOD17A3H MODIS/Terra Net Primary Production Yearly L4 Global 500m SIN Grid V006. NASA EOSDIS Land Processes DAAC (2015). doi:10.5067/MODIS/MOD17A3H.006.

[34] M. C. Hansen, P. V. Potapov, R. Moore, M. Hancher, S. A. Turubanova, A. Tyukavina, D. Thau, S. V. Stehman, S. J. Goetz, T. R. Loveland, A. Kommareddy, A. Egorov, L. Chini, C. O. Justice, J. R. G. Townshend, High-resolution global maps of 21st-century forest cover change., Science 342 (6160) (2013) 850–3. doi:10.1126/science.1244693.

[35] D. P. Roy, L. Boschetti, C. O. Justice, J. Ju, The collection 5 MODIS burned area product - Global evaluation by comparison with the MODIS active fire product, Remote Sensing of Environment 112 (2008) 3690–3707. doi:10.1016/j.rse.2008.05.013.

List of abbreviations and definitions

DLDD	Desertification, Land Degradation and Drought
LD	Land Degradation
LPD	Land Productivity Dynamics

List of Figures

List of Tables

LB-NA-28035-EN-N

JRC Mission

As the science and knowledge service of the European Commission, the Joint Research Centre's mission is to support EU policies with independent evidence throughout the whole policy cycle.

EU Science Hub
ec.europa.eu/jrc

@EU_ScienceHub

EU Science Hub - Joint Research Centre

Joint Research Centre

EU Science Hub

Publications Office

doi:10.2788/157180
ISBN 978-92-79-60680-9